Newton, D. L., Oldewurtel, M. D., Krinks, M. H., Shiloach, J., & Klee, C. B. (1984) *J. Biol. Chem. 259*, 4419-4426.
Olwin, B. B., & Storm, D. R. (1985) *Biochemistry 24*, 8081-8086.
Perrin, D. D., & Sayce, I. G. (1967) *Talanta 14*, 833-842.
Potter, J. D., & Gergeley, J. (1975) *J. Biol. Chem. 250*, 4628-4633.
Reid, R. E. (1983) *J. Theor. Biol. 105*, 63-76.
Reid, R. E., Gariépy, J., & Hodges, R. S. (1983) *FEBS Lett. 154*, 60-64.
Silver, P. J., Pinto, P. B., & Dachiw, J. (1986) *Biochem. Pharmacol. 35*, 2545-2551.
Steiner, R. F., Marshall, L., & Needleman, D. (1986) *Arch. Biochem. Biophys. 246*, 286-300.
Strynadka, N. C., & James, M. N. (1988) *Proteins 3*, 1-17.
Sundaralingam, M., Bergstrom, R., Strasburg, G., Rao, S. T., Roychodhury, P., Greaser, M., & Wang, B. C. (1985) *Science 227*, 945-948.
Weiss, B., & Levin, R. M. (1978) *Adv. Cyclic Nucleotide Res. 9*, 285-303.
Winkler, M. A., Fried, V. A., Merat, D. L., & Cheung, W. Y. (1987) *J. Biol. Chem. 262*, 15466-15471.
Wyman, J. (1964) *Adv. Protein Chem. 19*, 223-286.

Thermal Denaturation of the Ca^{2+}-ATPase of Sarcoplasmic Reticulum Reveals Two Thermodynamically Independent Domains†

James R. Lepock,* A. Michael Rodahl, Ching Zhang, Miriam L. Heynen, Brenda Waters, and Kwan-Hon Cheng‡
Guelph-Waterloo Program for Graduate Work in Physics, Waterloo Campus, University of Waterloo, Waterloo, Ontario N2L 3G1, Canada

Received July 12, 1989; Revised Manuscript Received August 30, 1989

ABSTRACT: Inactivation of Ca^{2+} uptake and ATPase activity of the Ca^{2+}-ATPase of rabbit sarcoplasmic reticulum was measured and compared to the thermal denaturation of the enzyme as measured by differential scanning calorimetry (DSC) and fluorescence spectroscopy. Two fluorophores were monitored: intrinsic tryptophan (localized in the transmembrane region) and fluorescein isothiocyanate (FITC)-labeled Lys-515 (located in the nucleotide binding domain). Inactivation, defined as loss of activity, and denaturation, defined as conformational unfolding, were irreversible under the conditions used. Activation energies (E_A) and frequency factors (A) for inactivation were obtained for the enzyme in 1 mM EGTA and 1 mM Ca^{2+}. These were transformed to a transition temperature for inactivation, T_m (defined as the temperature of half-inactivation when temperature is scanned upward at 1 °C/min). All denaturation profiles were fit with an irreversible model to obtain E_A and T_m for each transition, and the values of these parameters for denaturation were compared to the values for inactivation. In EGTA, denaturation obeys a single-step model (T_m = 49 °C), but a two-step model is required to fit the DSC provile of the enzyme in 1 mM Ca^{2+}. The specific locations of tryptophan and the fluorescein label were used to demonstrate that denaturation in Ca^{2+} occurs through two distinct thermodynamic domains. Domain I (T_m = 50 °C) consists of the nucleotide binding region and most likely the phosphorylation and transduction regions [MacLennan, D. H., Brandl, C. J., Korczak, B., & Green, N. M. (1985) *Nature 316*, 696-700]. Domain II (T_m = 57-59 °C) consists of the transmembrane region and probably the stalk region. Inactivation of ATPase activity and Ca^{2+} uptake when heated in 1 mM Ca^{2+} is due to denaturation of domain I. Inactivation of ATPase activity (T_m = 49 °C) when heated in 1 mM EGTA is also due to denaturation of domain I, but inactivation of Ca^{2+} uptake (T_m = 37 °C), yielding uncoupling of Ca^{2+} uptake from hydrolysis of ATP, does not correlate with any conformational change in the Ca^{2+}-ATPase detectable by these methods. From these results, it can be inferred that the conformational change occuring during the $E_2 \rightarrow E_1$ transition occurs primarily in domain II (ΔT_m = 8-10 °C), although there is a small stabilization of domain I (ΔT_m = 1 °C), demonstrating interaction and communication between these domains which is necessary for Ca^{2+}-dependent ATPase activity.

The Ca^{2+}-ATPase of sarcoplasmic reticulum (SR) pumps Ca^{2+} using energy derived from the hydrolysis of ATP. These two functions are not inseparable since many treatments uncouple Ca^{2+} transport from ATP hydrolysis, apparently without increasing membrane permeability (Berman, 1982). The ATP binding and phosphorylation sites and the Ca^{2+} binding sites are in diffferent secondary structural domains, as predicted from the primary sequence, but the location of these sites in the tertiary structure is unknown (MacLennan et al., 1985; Brandl et al., 1986; Clarke et al., 1989). Some forms of uncoupling appear to be due to conformational changes in the protein (Berman, 1982), suggesting that the ATPase and Ca^{2+}-translocation activities are located in discrete domains. Ca^{2+} uptake is inactivated rapidly at modest temperatures (near 37 °C) in EGTA while ATPase activity is unaffected at this temperature (McIntosh & Berman, 1978). Addition of Ca^{2+} protects against inactivation of Ca^{2+} uptake. The precise mechanism of inactivation and uncoupling is unknown (Berman, 1982).

The technique of thermal analysis has been profitably applied to the study of many materials, including macromolecules (Donovan, 1984). The general approach is to monitor tran-

†Supported by USPHS Grant CA40251 awarded by the National Cancer Institute, DHHS, to J.R.L. and by grants from the Natural Sciences and Engineering Research Council of Canada.
‡Present address: Department of Physics, Texas Tech University, Lubbock, TX 79409.

0006-2960/90/0429-681$02.50/0

sitions as a function of temperature. For macromolecules such as proteins, this allows the determination of the extent of denaturation or unfolding of the entire protein or specific domains (Privalov, 1982). Any phsyical technique that accurately reflects the extent of unfolding can be used, but differential scanning calorimetry (DSC) is most commonly employed. Information regarding the presence of domains, the strength of the interactions between domains, and the effects of the binding of ligands or substrate on domain stability and interactions can be determined from thermal analysis. Under favorable conditions, a low-resolution picture of a complex macromolecule can be obtained (Tsalkora & Privalov, 1985).

We have applied thermal analysis to the study of the domain organization and thermal inactivation of the Ca^{2+}-ATPase of rabbit SR. Thermal inactivation of Ca^{2+} uptake and ATPase activity was measured as a function of temperature in the presence and absence of Ca^{2+} and compared to the thermal denaturation determined by differential scanning calorimetry and fluorescence spectroscopy. Measurements of the fluorescence emission of intrinsic tryptophan and fluorescein isothiocyanate (FITC) labeled enzyme were used to determine the extent of denaturation of the protein domains containing these fluorophores.

Materials and Methods

Sarcoplasmic Reticulum Isolation and Calcium Uptake and ATP Hydrolysis Activities. Sarcoplasmic reticulum (SR) was isolated from the hind leg and back muscles of New Zealand White rabbits essentially as described by Eletr and Inesi (1972). Dithiothreitol at 1 mM was present throughout. The light SR fraction (LSR), which originates in elements of the longitudinal reticulum and is enriched in the Ca^{2+}-ATPase, was further isolated by using a sucrose density gradient essentially as described by Campbell et al. (1980). The SR banding at the 28–32% sucrose interface was defined as the LSR fraction. SDS-PAGE (Laemmli, 1970) was used to assess the purity of the Ca^{2+}-ATPase of each isolation.

Calcium-dependent ATPase (Ca^{2+}-ATPase) activity was assayed by monitoring the absorbance of NADH (λ = 340 nm) using an ATP-regenerating, coupled enzyme system similar to that described by Warren et al. (1974) containing 100 mM KH_2PO_4, 5 mM $MgSO_4$, 50 μM $CaCl_2$, 1 mM ATP, 125 μg/mL phosphoenolpyruvate, 8.5 μg/mL lactic acid dehydrogenase, 5 μg/mL pyruvate kinase, 300 μg/mL NADH, and LSR (3–14 μg of protien/mL), pH 7.0. Calcium uptake (Ca^{2+} uptake) was measured by monitoring the absorbance of arsenazo III (λ = 660 nm) as described by Herbette et al. (1972) in a solution of 100 mM KH_2PO_4, 5 mM $MgSO_4$, 50 μM $CaCl_2$, 0.4 mM ATP, 100 μM arsenazo III, and LSR (14 μg of protein/mL) pH 7.0. Some experiments were repeated using antipyrylazo III (75 μM) as an indicator of Ca^{2+} concentration in place of arsenazo III. In addition, a complete inactivation study of Ca^{2+} uptake was done by replacing the KH_2PO_4 with 100 mM KCl and using 10 mM potassium oxalate as a precipitating agent. Ca^{2+} uptake and ATPase activity in 1-mL cuvettes were initiated by adding either ATP or LSR, respectively.

Thermal Inactivation. The LSR at 600–700 μg of protein/mL was heated in a solution of 100 mM KCl, 5 mM dithiothreitol, pH 7.0, and either 1 mM $CaCl_2$ or 1 mM EGTA. The LSR at twice the concentration desired was added to a preheated test tube at the inactivation temperature containing an equal volume of the same solution. In this way, thermal equilibrium was achieved in 1–2 min. Samples wre removed at regular intervals and immediately added to the appropriate activity solution. Activity was derived from the slope of the linear region of each curve of arsenazo III, antipyrylazo III, or NADH absorbance. Both Ca^{2+} uptake and ATPase activity were directly proportional to the amount of LSR added over the range of activities measured. The rate of inactivation was obtained from a least-square analysis of the plot of ln activity vs time at the elevated temperature. The activation energy (E_A) and constant A of the Arrhenius relation (see below) were obtained from the slope and intercept of an Arrhenius plot.

Ca^{2+} Leakage. The rates of Ca^{2+} leakage at temperatures from 24 to 42 °C were measured by using LSR passively loaded with $^{45}Ca^{2+}$. The LSR (10 mg/mL) was loaded by incubation in 1 mM $^{45}CaCl_2$, 100 mM KCl, andd 10 mM TES at pH 7.0 for 1.5 h at 24 °C essentially as described in Meissner et al. (1986). Leakage was determined by measuring the calcium retained as a function of time after dilution (1:100) into release medium (100 mM KCl, 5 mM $MgCl_2$, 1 mM EGTA, and 10 mM TES at pH 7.0) at temperatures from 24 to 42 °C. Aliquots of 1 mL were removed as a function of time and filtered through 0.45-μm HAWP Millipore filters. The filters were washed with 10 mL of stop medium (release medium containing 10 μM Ruthenium Red) and counted in CytoScint (ICN). The decay curves of Ca^{2+} retained as a function of time were fit with the multiexponential function $A(t) = A_1e^{-k_1t} + A_2e^{-k_2t} + A_0$ where A_1 and A_2 are fractional components with rate constants of leakages k_1 and k_2. A_0 is a minor component with a leakage rate too small to be measured over the time course of the experiment (10 min).

Differential Scanning Calorimetry. A Microcal-2 differential scanning calorimeter (DSC) interfaced to a DEC Pro 380 computer was used to obtain all scans. The protein content of the LSR samples was 2–5 mg/mL, and a scan rate of 1 °C/min was used. For the DSC studies, the LSR was suspended in the same solutions used for thermal inactivation. The noisier scans were smoothed by a polynomial least-squares procedure. The baseline was corrected in two steps. First, the base line of the Ca^{2+}-ATPase scan was linearized by subtracting the instrumental base line (inactivation solution in both sample and reference cells) below approximately 30 °C, the rescan above approximately 65 °C, and a base line generated from a linearly varying proportion of the two between 30 and 65 °C. The procedure suggested by Hemmlinger and Höhne (1984) was used to further correct for the increase in specific heat (ΔC_p) upon denaturation by employing a correction factor proportional to the extent of the transition completed.

The algorithm proposed by Friere and Biltonen (1978), modified by Filimonov et al. (1982), was used for all curve fitting assuming reversible denaturation. The fit for irreversible denaturation was done as described below. The temperature dependence of a denaturation process obeying the Arrhenius relation can be approximated by

$$k(T) = e^{A-E_A/RT} \quad (1)$$

where k is the rate of denaturation, E_A the activation energy, and A a constant containing the entropy of inactivation. Irreversible denaturation, following pseudo-first-order kinetics, at a constant temperature as a function of time is described by the differential equation:

$$df_D(t)/dt = k(T)[1 - f_D(t)] \quad (2)$$

where f_D is the fraction denatured, T the temperature, and t the time. If the temperature is no longer constant, then the function $f_D[T(t)]$ as a function of time while temperature is scanned at a constant rate is found by replacing k in eq 2 with

the Arrhenius relation (eq 1) and letting $T = T_0 + vt$ where v is the scan rate and T_0 the starting temperature. The resulting equation:

$$df_D[T(t)]/dt = e^{A-E_A/R(T_0+vt)}(1 - f_D[T(t)]) \quad (3)$$

can be solved by numerical integration.

The excess specific heat is obtained from

$$C_p^{ex}(T) = m\frac{df_D}{dT} = \frac{m}{v}k(T)[1 - f_D(T)] \quad (4)$$

where m is a proportionally constant equal to the calorimetric enthalpy (ΔH_c). The above equation was used to generate the DSC profile for irreversible denaturation. The best-fit values of E_A, A, and ΔH_c were obtained by using the Simplex nonlinear curve-fitting algorithm (Nelder & Mead, 1965). A version of the computer program of Caceci and Cacheris (1984), modified to speed convergence and test for uniqueness, was used for fitting.

The approximations described by Fujita et al. (1979) were used to simplify the procedure for determining C_p^{ex}, and this approach was used for fitting all DSC scans containing multiple peaks. An approximate analytical solution for $f_D[T(t)]$ in eq 3 is obtained:

$$f_D[T(t)] = 1 - \exp\left\{\frac{-RT_c^2}{E_A v}\exp\left[\frac{E_A}{RT_c^2}(T - T_c)\right]\right\} \quad (5)$$

where T_c is the temperature at which $k = 1$. Briefly, the equation for temperature is written as $T(t) = T_c + v(t - t_0)$ where $T_c = T(t_0)$ so that $T_c = E_A/AR$. Then the Arrhenius relation has the form

$$k(T) = e^{A-E_A/R[T_c+v(t-t_0)]}$$

For $v(t - t_0) \ll T_c$, the term $t - t_0$ can be expanded in a Taylor series and higher order terms neglected [which is justified since $v(t - t_0)$ is less than 0.06 of T_c over the transition range of the Ca^{2+}-ATPase], giving

$$k(t) = e^{E_A v(t-t_0)/RT_c^2}$$

This is substituted into eq 2 which can now be solved exactly to give eq 5. This derivation is described in detail by Frujita et al. (1979), although their equations are in a different form, and an equivalent approach has recently been described by Sánchez-Ruiz et al. (1988). These approximations eliminate the necessity of numerical integration of eq 3 and speed up calculations considerably. E_A, A, and ΔH_c were still obtained from curve fitting by using the Simplex algorithm. The transition temperature (T_m) is defined as the temperature at which $f_D = 0.5$. The solution of eq 3 by numerical integration and the approximate solution (eq 5) give similar values for E_A, A, and ΔH_c. For DSC scans with profiles similar to those obtained for the Ca^{2+}-ATPase, T_m, calculated by the two methods, differs by less than 0.2 °C for curves for which E_A is greater than 300 kJ/mol.

Fluorescence Spectroscopy. Fluorescence spectra and intensities were obtained with an SLM 4800S spectrofluorometer interfaced to a DEC Pro 380 computer. LSR was suspended at 0.2 mg of protein/mL in the same solutions used for thermal inactivation and the DSC studies. The temperature of the samples was varied by increasing the temperature of a water bath used to control the cuvette holder temperature at 1 °C/min. The temperature of the sample lagged the water bath temperature by several degrees but increased at 0.9–1.0 °C/min. Aggregation tended to occur above 50 °C, but the effects were minimized by constantly stirring the solution in the cuvette. The increase in light scattering upon aggregation was less than 2% of the fluorescence emission. Intrinsic protein fluorescence was measured by using an excitation wavelength of 290 nm and an emission wavelength of 340 nm. Approximately 8 s, during which time the temperature changed by less than 0.15 °C, was required for each intensity measurement.

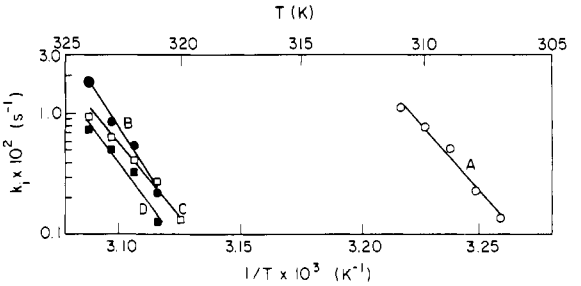

FIGURE 1: Arrhenius plots of the inactivation of (A) Ca^{2+} uptake in 1 mM EGTA (○), (B) Ca^{2+} uptake in 1 mM Ca^{2+} (●), (C) ATPase activity in 1 mM EGTA (□), and (D) ATPase activity in 1 mM Ca^{2+} (■).

The Ca^{2+}-ATPase was labeled with fluorescein isothiocyanate (FITC) essentially as described by Mitchinson et al. (1982). LSR at 0.2–0.3 mg/mL protein in 100 mM KCl, 10 mM TES, 1 mM DTT, and 1 mM EGTA, pH 7.8, was labeled with FITC at 8 nmol/mg of protein at 22 °C for 30 min. This resulted in approximately 75% inhibition of ATPase activity. The labeled LSR was washed twice and resuspended in the inactivation solution at 0.2 mg/mL. Fluorescence intensity was measured at excitation and emission wavelengths of 490 and 520 nm, respectively, while the temperature of the sample was increased at 1 °C/min.

The values of E_A and A for denaturation were derived from the normalized curves of the change in fluorescence, ΔF, vs temperature by fitting these curves with eq 5. This was done assuming that fractional denaturation is directly proportional to ΔF.

Results

Thermal Inactivation. The thermal inactivation of Ca^{2+} uptake and ATPase activity, in the presence of 1 mM EGTA (no Ca^{2+}) and 1 mM Ca^{2+}, was measured as described under Materials and Methods. Inactivation obeyed pseudo-first-order kinetics, and the inactivation rates (k) were determined by linear regression analysis of the section of the curves for heating times greater than that necessary for thermal equilibration (less than 2 min). Arrhenius plots of the rate constants for inactivation of Ca^{2+} uptake and ATPase activity are shown in Figure 1. The values of E_A and A, obtained by linear regression analysis, are given in Table I. The activation energies for thermal inactivation of both Ca^{2+} uptake and ATPase activity are all very high (404 to 573 kJ/mol), well into the range of activation energies normally observed for protein denaturation.

Ca^{2+} uptake is extremely sensitive to inactivation in EGTA compared to ATPase activity, as has been previously observed (MacIntosh & Berman, 1978). Addition of 1 mM Ca^{2+} shifts inactivation to higher temperatures by about 13 °C. ATPase activity is also stabilized by Ca^{2+} but to a lesser extent; the ATPase inactivation curve is shifted approximately 1 °C. The difference in sensitivity of Ca^{2+} uptake and ATPase activity to thermal inactivation and the difference in degree of Ca^{2+} stabilization suggest a differential thermal sensitivity of at least two regions or domains in the protein.

These results were verified by using antipyrylazo III since arsenazo III inhibits Ca^{2+} uptake and ATPase activity (Riollet & Champeil, 1987). However, the magnitude of inhibition by arsenazo III is constant for control and thermally inacti-

Table I: Thermodynamic Parameters for Irreversible Thermal Inactivation and Denaturation of Ca^{2+}-ATPase

thermal inactivation	E_A (kJ/mol)[a]	A[a]	T_m (°C)[b]	domain[e]
Ca^{2+} uptake, EGTA[f]	404 ± 34[i]	152 ± 13	36.6 ± 0.3	unknown
Ca^{2+} uptake, Ca^{2+}[f]	573 ± 31	209 ± 12	49.2 ± 0.3	I
ATPase, EGTA	423 ± 35	152 ± 13	49.2 ± 0.3	I
ATPase, Ca^{2+}	521 ± 62	189 ± 23	49.9 ± 0.5	I

denaturation DSC[g]	E_A (kJ/mol)[a]	A[a]	ΔH_c (J/g)[c]	T_m (°C)[b]	domain[e]
transition C, EGTA	413 ± 15[j]	149 ± 5	15.5 ± 1.8	48.3 ± 0.1	I, II
transition C, EGTA (FITC labeled)				49.7 ± 0.4	I, II
transition C, EGTA (1 mg/mL deoxycholate)	428	157	14.5	44.5	I, II
transition C, Ca^{2+}	581 ± 15	212 ± 6	11.8 ± 2.7	49.2 ± 0.2	I
transition D, Ca^{2+}	325 ± 29	113 ± 12	4.1 ± 1.0	56.9 ± 0.7	II

fluorescence[h]	E_A (kJ/mol)[a]	A[a]	ΔF_f (%)[d]	T_m (°C)[b]	domain[e]
Trp, EGTA	419 ± 100	166 ± 50	11.4 ± 2.0	48.5 ± 0.4	II
Trp, Ca^{2+}	408 ± 69	143 ± 26	22.0 ± 10.7	58.4 ± 1.6	II
FITC, EGTA	424 ± 9	153 ± 3	39.2 ± 4.7	49.5 ± 0.8	I
FITC, Ca^{2+}	472 ± 15	170 ± 5	41.7 ± 6.4	51.0 ± 0.3	I

[a] E_A and A are the activation energy and intercept from an Arrhenius plot. [b] T_m, the temperature of half-inactivation or denaturation, was determined from E_A and A. [c] The calorimetric enthalpy (ΔH_c) was determined by DSC. [d] ΔF_f is the change in fluorescence upon denaturation. [e] Domain I or II represents the domain in the Ca^{2+}-ATPase with which each activity or transition is associated. [f] Either EGTA or Ca^{2+} was present at 1 mM. [g] Denaturation as determined by DSC. [h] Denaturation as determined by monitoring the intrinsic Trp fluorescence or the fluorescein fluorescence of FITC-labeled enzyme. [i] The errors for E_A and A for inactivation are the standard deviations for the slope and intercept of the Arrhenius plot. [j] The errors given for the parameters of denaturation are standard errors from at least three independent measurements.

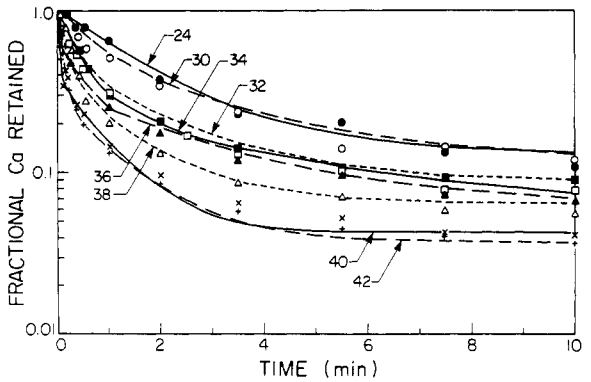

FIGURE 2: Normalized Ca^{2+} release curves in 1 mM EGTA as a function of time at 24–42 °C. The symbols are the experimental points [(●) 24 °C, (○) 30 °C, (■) 32 °C, (□) 34 °C, (▲) 36 °C, (△) 38 °C, (×) 40 °C, (+) 42 °C], and the lines are the best-fit curves determined as described under Materials and Methods.

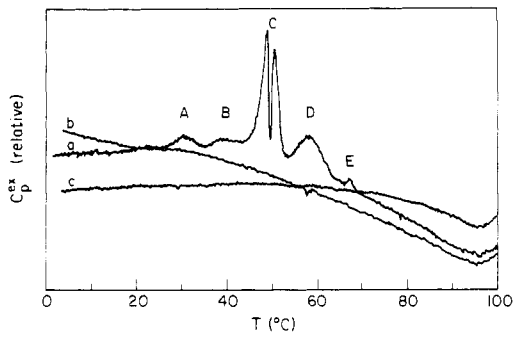

FIGURE 3: DSC scans of (a) LSR in 1 mM Ca^{2+}, (b) a rescan, and (c) an instrumental base line at a scan rate of 1 °C/min. The protein concentration was 2.5 mg/mL, and Ca^{2+}-ATPase purity was 87%.

vated LSR, allowing calculation of relative rates of uptake. The coupling ratio of Ca^{2+} accumulated to ATP consumed was always between 1 and 1.6 for control LSR whether measured with arsenazo III or antipyrylazo III. Rates of inactivation determined by using the two dyes were also similar. In addition, for some experiments, potassium oxalate (10 mM) was used in place of potassium phosphate (100 mM) to augment Ca^{2+} loading. Identical inactivation rates were obtained with both compounds. Ca^{2+} loading did not exceed 3 μmol of Ca^{2+}/mg of protein, and there was no evidence of vesicle rupture. The loading capacity of SR is limited and is approximately 4–6 μmol of Ca^{2+}/mg of protein for canine cardiac SR (Fehr & Lipford, 1985).

The simplest explanation for the greater thermal sensitivity of Ca^{2+} uptake when heated in EGTA is that the membrane becomes leaky to Ca^{2+} by some undefined mechanism, resulting in uncoupling. Rates of Ca^{2+} leakage in 1 mM EGTA were determined from 24 to 42 °C. The leakage curves are shown in Figure 2. Leakage is not pseudo first order but is multiexponential and increases somewhat with increasing temperature. In addition, a small fraction (4–10%) of the total Ca^{2+} taken up was not released or was released with a very long half-time compared to the length of the experiment. This can be seen by the plateau in the curves at 8–10 min. Thus, a double-exponential fit with a constant component of the form $A(t) = A_1e^{-k_1t} + A_2e^{-k_2t} + A_0$ was used for fitting. The leakage rate of the faster leaking component, comprising 60–70% of the total Ca^{2+}, is represented by k_1 and that of the slower leaking component (25–35%) by k_2. A reasonable fit was obtained with this function; however, it is more likely that there is a distribution of components rather than just three contributing to leakage. Thus, this type of fit is an oversimplification, but useful kinetic information is contained in k_1 and k_2.

The rate constants k_1 and k_2 plot as straight lines on Arrhenius plots (not shown) with activation energies of 105 ± 17 and 7 ± 12 kJ/mol, respectively. The value of E_A for k_1 is 4-fold less than that for inhibition of Ca^{2+} uptake, and E_A for k_2 is 40-fold less, although not significantly different from zero, suggesting that a simple increase in permeability to Ca^{2+}, as measured by this type of leakage experiment, is not responsible for inhibition of Ca^{2+} uptake.

Differential Scanning Calorimetry. Thermal denaturation was determined by DSC in order to ascertain if thermal inactivation is due to denaturation of the Ca^{2+}-ATPase. The LSR fraction is enriched in the Ca^{2+}-ATPase and was used for all denaturation and inactivation experiments (Campbell et al., 1980). The purity of the Ca^{2+}-ATPase was determined by SDS–PAGE for each isolation and ranged from 75 to 95% (usually 85–92%). Greater than half of the remaining protein consisted of calsequestrin, apparent $M_r \simeq 60000$ at pH 6.8, and the M_r 55000 protein (Campbell, 1986). The rest consisted of 10–12 minor proteins that were invisible by eye on

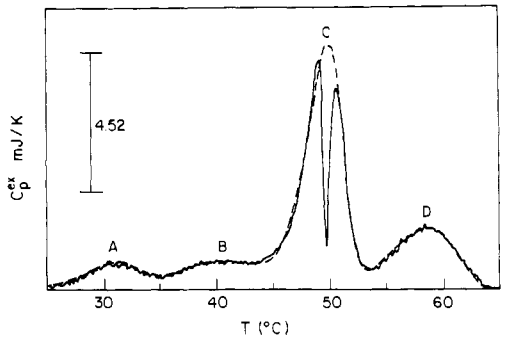

FIGURE 4: DSC scan of LSR in 1 mM Ca^{2+} corrected for the base line (original, Figure 3). The dashed line is the best fit for the four components assuming irreversible denaturation of each. The data points on the exothermic dip of transition C were removed before fitting. The respective fitting parameters [E_A (kJ/mol), A, and ΔH_c (J/g)] are the following: transition A, 350, 133, 1.78; transition B, 250, 90.3, 3.91; transition C, 570, 208, 11.8; transition D, 350, 122, 6.07. The bar in this and subsequent figures represents the calibration factor in millijoules per degrees kelvin.

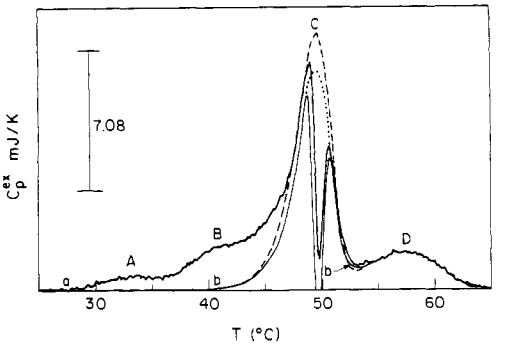

FIGURE 5: DSC scans of LSR in 1 mM Ca^{2+} (purity 79%): (a) control and (b) after heating at 42.5 °C for 1 h. The dashed and dotted lines (only shown where they differ from the original scans) are the best fits for the sum of transitions C and D for curves a and b, respectively. The respective fitting parameters [E_A (kJ/mol), A, and ΔH_c (J/g)] are as follows: curve a, transition C, 600, 219, 11.7; transition D, 300, 104, 3.82; curve b, transition C, 600, 219, 10.1; transition D, 300, 104, 3.83.

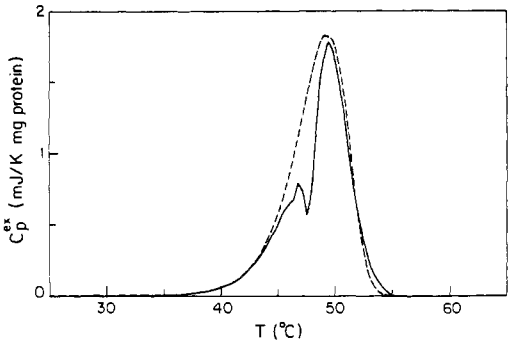

FIGURE 6: DSC scan of LSR in 1 mM EGTA (no Ca^{2+}) corrected for the base line. The dashed line is the best fit assuming irreversible denaturation. The purity of the Ca^{2+}-ATPase was greater than 95%, and transitions A and B are not present. The fitting parameters [E_A (kJ/mol), A, and ΔH_c (J/g)] are 400, 144, and 15.8, respectively.

the gels and detectable only by laser densitometry.

A DSC scan of LSR in 1 mM Ca^{2+} is shown in Figure 3. Five peaks (A–E) are usually observed with the amplitude of peaks A and B variable. No peaks are visible on the rescan; thus, all transitions are irreversible after heating to 100 °C. Evidence will be given that the doublet appearance of transition C is actually due to a sharp, exothermic transition superimposed on the endothermic transition C.

The rescan is flat with no evidence of a reversible transition that could be attributed to a lipid transition above 2 °C. These scans are of very high sensitivity and are inconsistent with the proposal that the break in the Arrhenius plot of ATPase activity at about 18 °C is caused by a lipid transition (Inesi et al., 1973).

Figure 4 is the same scan shown in Figure 3 corrected for the base line. The best-fit curve, consisting of four transitions (A–D), was generated by the method employing the Simplex algorithm described under Materials and Methods assuming irreversible denaturation and the presence of a superimposed exotherm on transition C. Thus, each peak is assumed to represent a single-step, endothermic, irreversible transition of the form N → D.

Transitions A and B do not represent components necessary for Ca^{2+} uptake or ATPase activity. A sample of LSR (Figure 5, curve a) was heated in 1 mM Ca^{2+} for 1 h at 42.5 °C and then scanned (Figure 5, curve b). Transitions A and B were not present after heating at 42.5 °C. The enthalpy of transition C decreased by 15%, and the rate of both ATPase activity and Ca^{2+} uptake decreased by 12 ± 4%. This reduction in activity correlates with the decrease in the enthalpy of transition C, but the complete irreversible denaturation of components A and B has no effect on Ca^{2+} uptake or ATPase activity. The predicted inactivations, determined from the values of E_A and A given in Table I for inactivation of Ca^{2+} uptake and ATPase activity using eq 1 and 2, are 19% and 16% for Ca^{2+} uptake and ATPase activity, respectively. The agreement between measured and predicted inactivation is good, and the minor differences between these values are probably due to the large extrapolation required to calculate the inactivation rate at 42.5 °C from E_A and A determined at 47–51 °C. Transitions A and B may represent protein damaged during isolation, protein destabilized by the salt solution used for heating, or protein that requires a factor for stabilization that is lacking in the inactivation solutions.

The DSC scan of the LSR in EGTA (Figure 6) is different from that obtained in the presence of Ca^{2+} (Figures 4 and 5). Transition D is not present, and transition C is centered about 1 °C lower. Transitions A and B are not present in this scan, but this sample of LSR has a very high purity of Ca^{2+}-ATPase (greater than 95% of the total protein). No transitions of any sort are detectable from 30 to 40 °C, the temperature range over which inactivation of Ca^{2+} uptake occurs in EGTA. For this particular scan, the exothermic transition is smaller than normal.

The temperature of the exotherm superimposed on transition C varied considerably, although it was usually found between 47 and 50 °C. It often passed well below the base line (negative C_p), suggesting that it is an exothermic event and that transition C is not composed of two separate transitions. The amplitude was also variable. The doublet structure was not observed using the fluoresence technique for measuring denaturation, implying an exothermic event occurring at 47–50 °C detectable by DSC alone. In addition, the inactivation of Ca^{2+} uptake and ATPase activity is inconsistent with two transitions. Thus, we infer that the dip is a superimposed exotherm. All curve fitting of transition C used only the beginning and ending of the peak; the points through the exotherm were ignored. All calculations of the thermodynamic parameters were made from the fitted curve, not the original.

The exothermic transition does not occur for LSR solubilized in the detergent deoxycholate (Figure 7). In deoxycholate containing 1 mM EGTA, only a single peak occurs with a T_m of 44.5 °C but with an E_A (428 kJ/mol) nearly identical with that obtained for transition C assuming that the dip is a superimposed exotherm. The decrease in T_m to 41

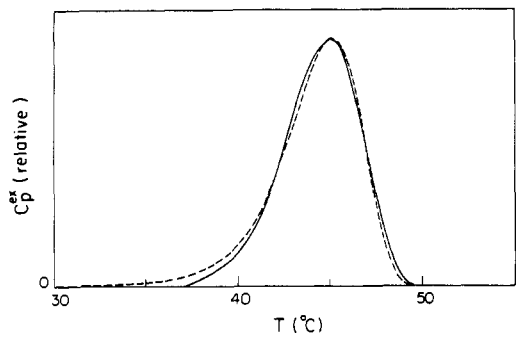

FIGURE 7: DSC scan of LSR in deoxycholate (1 mM EGTA, 1 mg/mL deoxycholate, and 2.42 mg/mL protein). The dashed line is the best fit with fitting parameters [E_A (kJ/mol) and A] of 428 and 157, respectively.

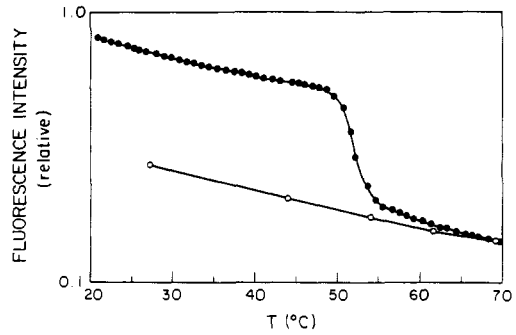

FIGURE 8: Fluorescence intensity (relative) of FITC-labeled LSR in 1 mM Ca^{2+} as a function of temperature increased at 1 °C/min. The lower curve (open symbols) was obtained on cooling.

°C is due to destabilization of the protein by the deoxycholate. Analysis of denaturation of the deoxycholate-solubilized LSR by Trp and FITC fluorescence also gives a T_m of approximately 41 °C (results not shown).

The exact nature of this exothermic transition is unknown. The sharpness of the exotherm indicates a controlling, rate-limiting step of high cooperativity which suggests the involvement of several Ca^{2+}-ATPase molecules. Membrane proteins are known to aggregate upon denaturation (Lysko et al., 1981), which would explain the cooperativity and exothermic nature of the transition. Gutiérrez-Merino et al. (1989) have also detected an exotherm in SR membranes which they attribute to protein aggregation.

These results indicate that the Ca^{2+}-ATPase denatures through two steps in 1 mM Ca^{2+} represented by transitions C and D and through a single step in 1 mM EGTA. There are two possible mechanisms to account for the two-step transition: (1) the protein undergoes two conformational unfoldings spread throughout; (2) two discrete domains unfold, each through a single step. DSC alone cannot differentiate between these possibilities. The fluorescence studies (below) show that the two transitions in 1 mM Ca^{2+} are due to the denaturation of two discrete domains.

Fluorescence Spectroscopy. Figure 8 is a plot of the fluorescence intensity of FITC-labeled LSR in 1 mM Ca^{2+} as a function of temperature increased at a rate of 1 °C/min, the same as for the DSC scans. FITC has been shown to label Lys-515 which is near the ATP binding site (Brandl et al., 1986). There is a nearly linear decrease in fluorescence as a function of increasing temperature, due to temperature-induced quenching, with a sharp, irreversible drop in intensity centered at about 50 °C. The curve obtained during cooling is flat, and the curve obtained during a second heating (not shown) falls upon the cooling curve. Similarly shaped curves were obtained for the intrinsic protein fluorescence, which is

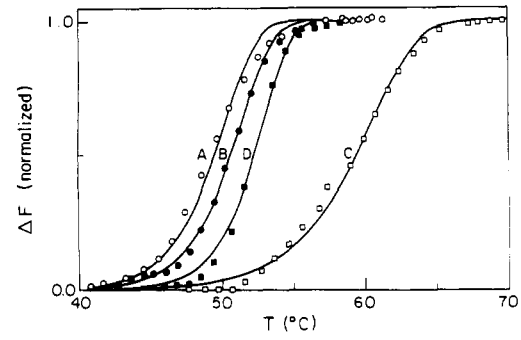

FIGURE 9: ΔF vs temperature for LSR heated at 1 °C/min: (A) intrinsic Trp fluorescence, 1 mM EGTA (○); (B) FITC-labeled Ca^{2+}-ATPase fluoresence, 1 mM EGTA (●); (C) intrinsic Trp fluorescence, 1 mM Ca^{2+} (□); (D) FITC-labeled Ca^{2+}-ATPase fluorescence, 1 mM Ca^{2+} (■). The symbols represent the measured values, and the solid lines are the fitted curves for irreversible denaturation.

dominated by Trp fluorescence in proteins containing Trp and Tyr (Cowgill, 1976). The secondary structural predictions of MacLennan et al. (1985) place 11 of 13 Trp in the transmembrane domain. One of the two Trp not in this domain is closely associated with it through the stalk domain. Thus, Trp fluorescence should preferentially probe the transmembrane domain.

The base line was corrected as described under Materials and Methods, and the resulting, normalized plot of the change in fluorescein fluorescence due to denaturation (ΔF) is shown in Figure 9, curve B. If denaturation is a simple two-state process and if the fluorescence of the native state differs from that of the denatured state, $\Delta F \propto f_D$ where f_D is the fraction denatured and the derivative (df_D/dT) should be proportional to C_p^{ex} as determined by DSC.

The fractional change in fluorescence (ΔF) of both intrinsic Trp and FITC-labeled Ca^{2+}-ATPase in 1 mM EGTA and 1 mM Ca^{2+} is given in Figure 9. The solid lines are the best fit to the measured values using the irreversible model. The fitting parameters E_A and A are given in Table I. The fractional denaturation in 1 mM EGTA has a similar temperature dependence (slope) whether determined from the decrease in Trp or fluorescein fluorescence, except that the curve for the FITC-labeled enzyme is shifted to higher temperatures by about 1 °C. This is due to a slightly greater stability of the FITC-labeled enzyme, since the denaturation temperature of the FITC-labeled Ca^{2+}-ATPase in 1 mM EGTA (transition C) determined by DSC is also higher (Table I).

In 1 mM Ca^{2+}, the denaturation temperature, determined from the change in fluorescein fluorescence, is shifted about 1 °C higher, as was found by DSC for transition C, but there is a 10 °C shift in the Trp curve. This is consistent with the DSC results which showed two distinct peaks in 1 mM Ca^{2+}. Thus, transition D is due to the denaturation of an independent domain monitored by the intrinsic Trp fluorescence. This will be referred to as domain II. The denaturation of domain I, which is monitored by the fluorescence of the FITC-labeled enzyme, yields transition C.

The value of the fractional decrease in fluorescence (ΔF_f) at each transition was found by extrapolating the base line above and below the transition back to the midpoint of the transition and measuring the difference at T_m. These values are given in Table I as the fraction of total fluorescence intensity at T_m. The magnitude of ΔF_f in 1 mM Ca^{2+} is greater than ΔF in EGTA. This difference between these two values is 10.6 ± 3.6% (SEM) of the total Trp fluorescence. The difference for the FITC-labeled enzyme, 2.5 ± 2.7%, is not

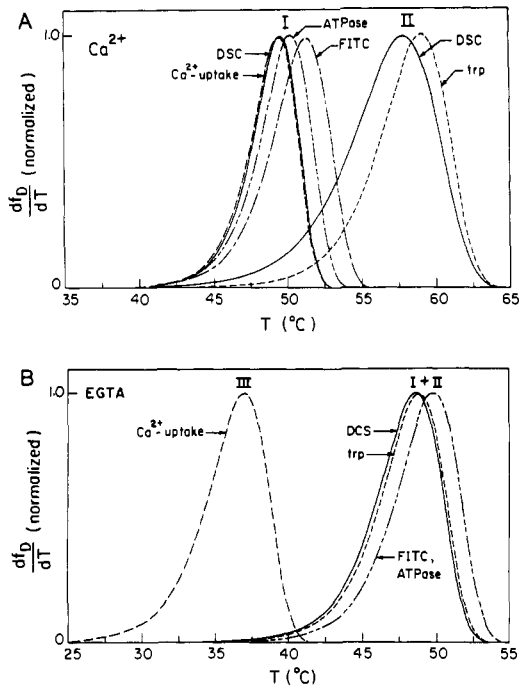

FIGURE 10: Curves of df_D/dT for inactivation of Ca^{2+} uptake and ATPase activity and denaturation determined by DSC and Trp and FITC fluorescence. All curves were generated from the fitting parameters (E_A and A) given in Table I and normalized. Panel A is for LSR in 1 mM Ca^{2+} and panel B in 1 mM EGTA.

statistically significant. Calcium binding increases Trp fluorescence by about 5% (Dupont et al., 1985), suggesting that the 11% difference in ΔF_f may be due to the Ca^{2+}-induced $E_2 \rightarrow E_1$ transition and that the final, denatured states of both enzyme conformations have similar fluorescence and a similar distribution of denatured conformations.

Correlation of Inactivation and Denaturation. The inactivation results, previously given as Arrhenius plots in Figure 1, are expressed in Figure 10 as the derivative of fractional inactivation as a function of temperature increased at 1 °C/min. The transformation uses eq 3 and 4 (described under Materials and Methods) and allows a direct comparison with C_p^{ex} determined from DSC and $d\Delta F/dT$ determined from fluorescence. These curves are completely described by an activation energy E_A, the constant A, and a scan rate of heating. This gives a transition temperature T_m (defined as the temperature of half-inactivation as for the curves of denaturation). These values are given in Table I. Since inactivation is a function of both temperature and time, equilibrium is never achieved, and the position of each curve is a function of the scan rate.

Ca^{2+} uptake, with a T_m of 36.6 °C, is very thermolabile when heated in 1 mM EGTA. Addition of Ca^{2+} shifts the T_m to 49.2 °C (ΔT_m =12.6 °C), indicating considerable stabilization. The temperature dependence of inactivation is somewhat higher as illustrated by the increase in apparent activation energy from 404 to 573 kJ/mol. In EGTA, ATPase activity (T_m = 49.2 °C) is much more resistant to inactivation than Ca^{2+} uptake. Thus, exposure to moderate temperatures uncouples Ca^{2+} uptake from ATPase activity. Addition of Ca^{2+} protects ATPase activity slightly from inactivation with the T_m increased by 0.7 °C to 49.9 °C.

In 1 mM Ca^{2+} (Figure 10A), transition C, which is identified as the denaturation of domain I, exactly matches inactivation of Ca^{2+} uptake. The T_m's are the same (49.2 °C) and the values of E_A, which is inversely proportional to the half-width of each curve, nearly identical (573–581 kJ/mol). The curve representing denaturation of domain I in the FITC-labeled enzyme has a slightly higher T_m (51.0 °C), due to stabilization at the ATP binding site. The T_m of inactivation of ATPase activity (49.9 °C) is slightly higher (ΔT_m = 0.7 °C) than that for Ca^{2+} uptake. This is a significant and highly reproducible difference. This can only be due to a partial refolding of domain I, implying some reversibility of denaturation of this domain.

The denaturation of domain II, represented by transition D in the DSC scan and observable by the drop in Trp fluorescence, occurs at 57–58 °C, above the temperature at which inactivation of Ca^{2+} uptake and ATPase activity occurs.

In 1 mM EGTA (Figure 10B), the Ca^{2+}-ATPase denatures as a single cooperative unit or domain. The T_m's from DSC (48.3 °C) and Trp fluorescence (48.5 °C) match almost exactly. In addition, there is an excellent match between the E_A's determined by these two techniques–413 and 419 kJ/mol, respectively. Denaturation determined by FITC has a slightly higher T_m of 49.5 °C due to FITC-induced stabilization. The T_m of inactivation of ATPase activity is again higher (ΔT_m = 0.9 °C) than the T_m of denaturation of this domain. The exact match between the curves of inactivation of ATPase activity and denaturation by FITC is probably fortuitous.

The inactivation of Ca^{2+} uptake (T_m = 36.6 °C) is extremely thermolabile and is not due to any large-scale denaturation or conformational change in the Ca^{2+}-ATPase detectable by DSC or Trp or FITC fluorescence.

The inactivation and denaturation measurements were made at different LSR concentrations (inactivation, 0.3 mg of protein/mL; fluorescence, 0.2 mg/mL; and DSC, 2–5 mg/mL). The excellent correlation between the T_m's determined by these techniques suggests that denaturation is independent of protein concentration. Two further experiments confirm this. To check for linearity, inactivation was measured at protein concentrations from 0.1 to 4 mg/mL with no difference in the rate of inactivation observed. DSC scans were obtained from 1 to 8 mg/mL, again with no change in T_m. In addition, measurements by Gutiérrez-Merino et al. (1989) show no apparent change in T_m with concentration. The reason for this is that the effective concentration of Ca^{2+}-ATPase is determined by the concentration of the protein in the membrane, which is much greater and dominates any change in concentration due to changes in LSR concentration.

Discussion

A simple two-state (one-domain) or three-state (two-domain) irreversible model is used for the analysis of the denaturation and thermal inactivation of the Ca^{2+}-ATPase in 1 mM EGTA or Ca^{2+}, respectively. The irreversible model was chosen since inactivation of Ca^{2+} uptake and ATPase activity is apparently irreversible under the conditions used for heating, necessitating an irreversible analysis of denaturation for direct comparison. In addition, it was not possible to fit most of the DSC scans assuming reversible denaturation without introducing additional transitions since the DSC profile of a reversible transition is skewed on the high-temperature side while the profile for transition C is skewed on the low-temperature side (see Figures 5–7).

Usually, considerable effort is expended to justify the assumption that reversibility holds during the transition for the analysis of DSC scans (Sturtevant, 1987). This aids in a rigorous thermodynamic analysis and in the deconvolution of multistep transitions (Friere & Biltonen, 1978; Privalov, 1982), but it is not necessary since transitions exhibiting irreversibility can also be deconvoluted, as shown here, although one must assume the number of transitions present.

A reversible transition exhibiting irreversibility can be modeled as a three state-transition of the form:

$$N \underset{k_{-1}}{\overset{k_1}{\rightleftharpoons}} D_R \xrightarrow{k_2} D_I$$

where D_R and D_I represent reversibly and irreversibly unfolded or denatured forms. We have simplified this to the two-state form, $N \xrightarrow{k} D$, since inactivation measurements give information only about irreversibility. The excellent correspondence between denaturation, measured by two independent techniques (DSC and fluorescence), and inactivation of Ca^{2+} uptake indicates that this assumption is appropriate, although the denaturation of domain I leading to inactivation of ATPase activity appears to be slightly reversible.

Which parts of the Ca^{2+}-ATPase correspond to domains I and II? MacLennan and co-workers have predicted the secondary structure and domain organization of the Ca^{2+}-ATPase based on the primary sequence (MacLennan et al., 1985; Brandl et al., 1986). They predict five structural domains. The transmembrane domain is thought to consist of 8 or 10 helices crossing the lipid bilayer. The stalk domain consists of five helices apparently coupled to the transmembrane domain. The nucleotide binding domain contains the ATP binding site, and Asp-351 in the phosphorylation domain is phosphorylated during ATP hydrolysis. Although it was originally proposed that the stalk region contains the high-affinity Ca^{2+} binding sites (MacLennan et al., 1985), recent work has shown that they are located in the transmembrane region (Clarke et al., 1989a,b). The polypeptide chain crosses the lipid bilayer between the transduction and phosphorylation domains. Twelve of the 13 Trp residues are in the transmembrane domain or associated with it; thus, this domain is preferentially probed by Trp fluorescence. The nucleotide domain is labeled by FITC at Lys-515 (Mitchinson, 1982).

The results from the studies with Trp fluorescence indicate that the transmembrane domain is part of domain II. Association of the nucleotide binding domain, and almost certainly the phosphorylation domain, with domain I can be inferred from FITC labeling. The ΔH_c of domain I is 74% of the total, suggesting that most of the protein is in this domain. The location of the transduction and stalk domains cannot be determined from these studies; however, one would expect the transduction domain to be part of domain I on the basis of the relative ΔH_c of each domain and an apparent strong interaction with the nucleotide binding domain (Inesi, 1985). Two of the five helices in the stalk region are continuous with the transmembrane helices in the secondary structural prediction (MacLennan et al., 1985), suggesting a strong association between these domains. There is no evidence to assign the α-helical subdomain (5.5% of the total residues) to either domain I or domain II.

The nucleotide binding, phosphorylation, and transduction domains comprise approximately 52% of the total amino acid residues. The enthalpy of transition C is 74% of the total. Thus, if this assignment is correct, the denaturation of domain II has a lower specific enthalpy than that of domain I. This is not surprising since most of the residues of domain II are buried in the lipid bilayer and presumably would not be exposed to the aqueous environment upon unfolding.

The observed denaturation partially explains functional inactivation at elevated temperature. The T_m for inactivation of ATPase activity in EGTA is 49.2 °C, very close to the T_m of denaturation of the Ca^{2+}-ATPase. Addition of 1 mM Ca^{2+} shifts the T_m by 0.7 °C, nearly identical with the 0.8–0.9 °C shift in the T_m of domain I. In both the absence and presence of Ca^{2+}, the activation energy for the denaturation of domain I is similar to the activation energy for the inactivation of ATPase activity. Thus, inactivation of ATPase activity in either the presence or the absence of Ca^{2+} is due to denaturation of domain I. This further supports the inclusion of the nucleotide binding domain in domain I. However, the 0.7–0.9 °C greater T_m for inactivation compared to denaturation implies that the denaturation of domain I is partially reversible.

Inactivation of Ca^{2+} uptake is not as straightforward. A T_m of 36.6 °C is predicted in EGTA. Nothing is observed at this temperature by DSC or FITC or Trp fluorescence, eliminating the involvement of the complete denaturation of either domain I or domain II. In 1 mM Ca^{2+}, the temperature dependence of inactivation of Ca^{2+} uptake is identical with the denaturation of domain I. Denaturation of domain II is not involved since its T_m is too high.

A potential mechanism, often proposed to account for uncoupling or low coupling ratios (Hasselbach, 1981), for the thermal inactivation of Ca^{2+} uptake in the absence of Ca^{2+} is an increase in membrane permeability to Ca^{2+}. This appears to be the mechanism of uncoupling by such agents as deoxycholate (MacLennan, 1970), ether (Fiehn & Hasselbach, 1969), and EGTA at high pH (Duggan & Martonosi, 1970). Other means of uncoupling, such as mild acid treatment (Berman et al., 1977) and EGTA at neutral pH (McIntosh & Berman, 1978), apparently do not increase membrane permeability. As shown by this study, uncoupling by EGTA is more accurately described as thermal inactivation in the absence of Ca^{2+} stabilization and has a different activation energy than that for Ca^{2+} leakage or release. In addition, the affinity for Ca^{2+} stabilization ($K_{0.5} = 4.9 \times 10^{-6}$ M) is very high (McIntosh & Berman, 1978) and of a similar magnitude to the affinity of the high-affinity Ca^{2+} binding sites on the Ca^{2+}-ATPase, suggesting protein involvement. Berman has proposed that these latter agents induce uncoupling by irreversibly altering the conformation of the Ca^{2+}-ATPase (Berman, 1982).

Further evidence for the direct involvement of protein in the thermal inhibition of Ca^{2+} uptake is the high activation energy for this process. We obtain a value of 409 kJ/mol. McIntosh and Berman (1978) report a high but slightly smaller value of 273 kJ/mol. These large values for the activation energy suggest a transition or conformational change as the rate-limiting step for uncoupling.

If this transition is a conformational change in the Ca^{2+}-ATPase, then it must be a very small structural change spread throughout the protein or a transition in a small domain of the protein not observable by Trp or FITC fluorescence and of very low enthalpy. Any structural change must occur without changes in secondary structure, since there are no gross changes in α-helical content, as detected by CD, upon uncoupling (Berman, 1980).

Any localized domain involved in uncoupling cannot be part of the transmembrane region or ATP binding domain since the denaturation temperature of these domains can be confidently determined from Trp or FITC fluorescence. If the nucleotide binding, phosphorylation, and transduction domains denature as a single cooperative unit, as suggested by the large enthalpy of transition C, then these domains cannot contain the uncoupling domain. A potential candidate is the α subdomain or hinge domain consisting of residues 680 to 720–740 (MacLennan et al., 1985; Brandl et al., 1986).

These results also shed some light on the structural change involved in the $E_2 \rightarrow E_1$ transition. Addition of Ca^{2+} shifts the Ca^{2+}-ATPase from the E_1 to the E_2 state detectable by an increase in Trp fluorescence (Dupont et al., 1985). The

extent or location of the conformational change cannot be determined from fluorescence alone. In addition, it is not possible to prove that the decrease in Trp fluorescence is not due to quenching by a close interaction between Ca^{2+} and the Trp residues. Evidence from CD implies that there is very little, if any change, in secondary structure during the $E_2 \rightarrow E_1$ transition (Nakamoto & Inesi, 1986). The differential stabilization of domain I and II by Ca^{2+} suggests that the conformational change in the transmembrane domain is much greater than that in the remainder of the protein and that the change in fluorescence is, indeed, due to a protein conformational change and not contact between Ca^{2+} and Trp. The conformational change from E_1 to E_2 is accompanied by a considerable stabilization of this region and a much smaller stabilization of the nucleotide binding, phosphorylation, and transduction domains. The weak stabilization implies a weak interaction between these two thermodynamically independent units (domains I and II); however, some interaction is necessary since ATPase activity is Ca^2 dependent, requiring communication between domains I and II.

Registry No. ATPase, 9000-83-3; Ca, 7440-70-2.

References

Berman, M. C. (1982) *Biochim. Biophys. Acta 694*, 95–121.

Berman, M. C., McIntosh, D. B., & Kench, J. E. (1977) *J. Biol. Chem. 252*, 994–1001.

Berman, M. C., Diamond, E. M., Norton, B., & McIntosh, D. B. (1980) in *Thermoregulatory Mechanisms and their Therapeutic Implications* (Cox, B., Lomax, P., Milton, A. S., & Schönbaum, E., Eds.) pp 130–132, S. Karger, Basel.

Brandl, C. J., Green, N. M., Korczak, B., & MacLennan, D. H. (1986) *Cell 44*, 597–607.

Caceci, M. S., & Cacheris, W. P. (1984) *Byte 9*, 340–362.

Campbell, K. P. (1986) in *Sarcoplasmic Reticulum in Muscle Physiology* (Entman, M. L., & Van Winkle, W. B., Eds.) pp 65–99, CRC Press, Boca Raton, FL.

Campbell, K. P., Franzini-Armstrong, C., & Shamoo, A. E. (1980) *Biochim. Biophys. Acta 602*, 97–105.

Clarke, D. M., Loo, T. W., Inesi, G., & MacLennan, D. H. (1989a) *Nature 339*, 476–478.

Clarke, D. M., Maruyama, K., Loo, T. W., Leberer, E., Inesi, G., & MacLennan, D. H. (1989b) *J. Biol. Chem. 264*, 11246–11251.

Cowgill, R. W. (1976) in *Biochemical Fluorescence Concepts* (Chen, R. F., & Edelhoch, H., Eds.) pp 441–486, Marcel Dekker, New York.

Donovan, J. W. (1984) *Trends Biochem. Sci. (Pers. Ed.) 9*, 340–344.

Duggan, P. F., & Martonosi, A. (1970) *J. Gen. Physiol. 56*, 147–167.

Dupont, Y., Bennet, N., Pougeois, R., & Lacapere, J.-J. (1985) in *Structure and Function of Sarcoplasmic Reticulum* (Fleischer, S., & Toromura, Y., Eds.) pp 225–248, Academic Press, Toronto.

Eletr, S., & Inesi, B. (1972) *Biochim. Biophys. Acta 282*, 174–179.

Feher, J. J., & Lipford, G. B. (1985) *Biochim. Biophys. Acta 818*, 373–385.

Fiehn, W., & Hasselbach, W. (1969) *Eur. J. Biochem. 9*, 574–578.

Filimonov, V. V., Potekhin, S. A., Matveev, S. W., & Privalov, P. L. (1982) *Mol. Biol. (Engl. Transl.) 16*, 551–562.

Friere, E., & Biltonen, R. L. (1978) *Biopolymers 17*, 463–479.

Fujita, S. C., Gu, N., & Imahori, K. (1979) *Biochemistry 18*, 24–28.

Gutiêrrez-Merino, C., Molinu, A., Escudero, B., Diez, A., & Laynez, J. (1989) *Biochemistry 28*, 3398–3406.

Hasselbach, W. (1981) in *Membrane Transport* (Bonting, S. L., & DePont, J. J., Eds.) pp 183–206, Elsevier/North-Holland Biomedical Press, Amsterdam.

Hemminger, W., & Höhne, G. (1984) *Calorimetry—Fundamentals and Practice* (Translated by Y. Goldman) Verlag Chemie GmbH, Weinheim.

Herbette, L., Marquardt, J., Scarpa, A., & Blasie, J. K. (1977) *Biophys. J. 20*, 245–272.

Inesi, G. (1985) *Annu. Rev. Physiol. 47*, 573–601.

Inesi, G., Millmam, M., & Eletr, S. (1973) *J. Mol. Biol. 81*, 483–504.

Laemmli, U. K. (1970) *Nature 227*, 680–685.

Lysko, K. A., Carlson, R., Taverna, R., Snow, J., & Brandts, J. F. (1981) *Biochemistry 20*, 5570–5576.

MacLennan, D. H. (1970) *J. Biol. Chem. 245*, 4508–4518.

MacLennan, D. H., Brandl, C. J., Korczak, B., & Green, N. M. (1985) *Nature 316*, 696–700.

McIntosh, D. B., & Berman, M. C. (1978) *J. Biol. Chem. 253*, 5140–5146.

Meissner, G., Darling, E., & Eveleth, J. (1986) *Biochemistry 25*, 236–244.

Mitchinson, C., Wilderspin, A. F., Trinnaman, B. J., & Green, N. M. (1982) *FEBS Lett. 146*, 87–92.

Nakamoto, R. K., & Inesi, G. (1986) *FEBS Lett. 194*, 258–262.

Nelder, J. A., & Mead, R. (1965) *Comput. J. 7*, 308–313.

Privalov, P. L. (1982) *Adv. Protein Chem. 35*, 1–104.

Riollet, S., & Champeil, P. (1987) *Anal. Biochem. 162*, 160–162.

Sânchez-Ruiz, J. M., Lôpez-Lacomba, J. L., Cortijo, M., & Mateo, P. L. (1988) *Biochemistry 27*, 1648–1652.

Sturtevant, J. M. (1987) *Annu. Rev. Phys. Chem. 38*, 463–488.

Tanford, C. (1984) *CRC Crit. Rev. Biochem. 17*, 123–151.

Tsalkora, T. N., & Privalov, P. L. (1985) *J. Mol. Biol. 181*, 533–544.

Warren, G. B., Toon, P. A., Birdsall, J. M., Lee, A. G., & Metcalfe, J. C. (1974) *Proc. Natl. Acad. Sci. U.S.A. 71*, 622–626.